

2(b). The experiments were not extended to obtain the data needed for a detailed description of these hysteretic properties of the oxidation processes.

¹³D. M. Newns, Phys. Rev. **178**, 1123 (1969).

¹⁴J. W. Gadzuk, J. K. Hartman, and T. N. Rhodin, Phys. Rev. B **4**, 241 (1971).

Screening of Wannier Exciton States near the Metal-Insulator Transition

Baruch Raz, Aharon Gedanken, Uzi Even, and Joshua Jortner

Department of Chemistry, Tel-Aviv University, Tel-Aviv, Israel

(Received 4 April 1972)

We provide a new spectroscopic criterion for the observation of the insulator-metal transition in a two-component system, which is based on the disappearance of Wannier exciton states in the metallic region. This effect has been observed in the vacuum-ultra-violet spectra of mercury/xenon mixtures deposited at 10–30°K, where the Xe Wannier states are abruptly washed out at (55 ± 5)% of Hg.

Metal-nonmetal transitions in ordered and disordered systems¹ have been experimentally induced by structural modifications,² by the application of external fields,³ by concentration changes in two-component systems,^{4–6} and by density changes in a one-component system.^{7,8} Most of these studies¹ monitored the electrical transport properties and the magnetic properties of the system undergoing the MNM transition. We advance a new spectroscopic criterion for the observation of the MNM transition. Wannier-Mott excitons in a two-component system, consisting of open-shell metallic atoms and of closed-shell saturated atoms, are utilized as a spectroscopic probe to monitor the MNM transitions. These large-radius excited states are expected to persist only in the insulating state, and become unbound in the metallic state because of short-range dielectric screening effects.

Our experimental approach is based on Mott's argument concerning the effects of long-range forces on the MNM transition.⁹ The long-range electron-hole potential in the nonmetallic state,

$$V(r) = -e^2/\mathcal{E}r \quad (1)$$

(where \mathcal{E} is the static dielectric constant), is replaced in the metallic state by a short-range potential, which according to the Thomas-Fermi prescription is

$$V(r) = -(e^2/\mathcal{E}r) \exp(-qr), \quad (2)$$

where the screening length is

$$q^2 = 4m^*e^2(3n/\pi)^{1/3}/\hbar^2\mathcal{E}, \quad (3)$$

with n corresponding to the free-electron density. As it is well known,⁹ the potential well (2) does

not have bound states for

$$qa_H > 1.0, \quad (4)$$

where the modified Bohr radius⁹ is $a_H = \hbar^2\mathcal{E}/m^*e^2$, while m^* represents the electron effective mass.

Consider the implications of these arguments for the description of Wannier-Mott-type shallow and deep exciton and impurity states.^{10,11} In a nonmetallic solid¹⁰ the Coulomb electron-hole attraction is dielectrically screened, whereupon for large-radius states the microscopic variation of the crystal and of the positive-hole potentials is replaced by Eq. (1). Furthermore, when the conduction band is wide and parabolic, the effects of the crystal potential can be subsumed into an effective mass.^{10,11} The envelope function for large-radius exciton and impurity states obeys the equation

$$[-(\hbar^2/2m^*)\nabla^2 + V(r) - E]\psi = 0, \quad (5)$$

where the potential is given by Eq. (1). A Rydberg series converging to the bottom of the conduction band has been experimentally observed for shallow states in semiconductors¹² and for deep-lying states in rare-gas solids.¹³ The observation of exciton states in dense rare gases is independent of symmetry arguments, and these excited states are amenable to experimental observation in positionally disordered systems (i.e., liquid rare gases)¹⁴ and in substitutionally disordered systems (i.e., heavily substituted rare-gas alloys).¹⁵ Now, when an insulator (such as a rare-gas solid) is gradually substituted by unsaturated metal atoms, this two-component system may eventually undergo a MNM transition, whereupon $V(r)$ in Eq. (5) will take the ap-

proximate form (2). Furthermore, when the screening length obeys Eq. (4) no bound excited Wannier states will exist any more.⁹ This effect has been experimentally observed by us in Xe/Hg mixed solids at low temperature.

We have studied the vacuum-ultraviolet absorption spectra (spectral region 1200–1600 Å) of Xe/Hg solid films at 10–40°K. Gaseous mixtures of Xe and Hg containing 0–0.8 mole fraction [i.e., (0–80)% mole percent] of Hg were prepared at a total pressure of 2×10^{-3} – 10^{-1} Torr at room temperature in a vacuum system previously pumped down to 2×10^{-7} Torr. The gaseous mixtures were condensed on a LiF window, mounted on a variable-temperature helium-flow cryostat. The Xe/Hg solid films were prepared at 40°K and measured at 10°K and at 40°K. From the known optical constants of pure Xe we estimate the thickness of the films to be ~ 100 Å. Samples at different compositions were deposited for different times (10 min for 15% Hg up to 100 min for 70% Hg) until the optical density in the relevant spectral region was 0.5–1.0. The sticking coefficients of both components at 40°K are close to unity, and no enrichment of the solid sample (relative to the gas-phase compositions) is expected.

The spectroscopic light sources were argon and krypton discharge lamps¹⁶ producing molecular continua in the range 1100–1600 Å. A 1-m normal incidence vacuum uv monochromator (McPherson 225) with a resolution of 3 Å was used. Single-beam photoelectric detection was employed using an EMI 9514 S photomultiplier and a sodium-salicylate converter.

In Fig. 1 we display the absorption spectra of Xe/Hg films. The spectrum of pure Xe exhibits the well-known¹³ Wannier exciton series [$n=1$ ($^2P_{3/2}$) state at 8.40 eV, $n=2$ ($^2P_{3/2}$) state at 9.08 eV, and $n=3$ ($^2P_{3/2}$) state at 9.22 eV], in accord with Baldini's original work.¹³ When the Hg concentration is increased in the range (15–40)% the Xe $n=1$ and $n=2$ states are well defined, apart from line broadening, which is attributed to the effects of substitutional disorder. The simple coherent-potential approximation¹⁷ predicts that for cellular disorder the optical line broadening in a binary alloy is proportional to $[X(1-X)]^{1/2}$, where X is the mole fraction of one of the components. The gradual increase in the width of the $n=1$ ($^2P_{3/2}$) and of the $n=2$ ($^2P_{3/2}$) Xe excitons in the range $X_{\text{Hg}}=(15-40)\%$ is qualitatively consistent with these expectations. Furthermore, provided that the system is nonmetallic, we expect a minor change in the Xe linewidths in the concentration

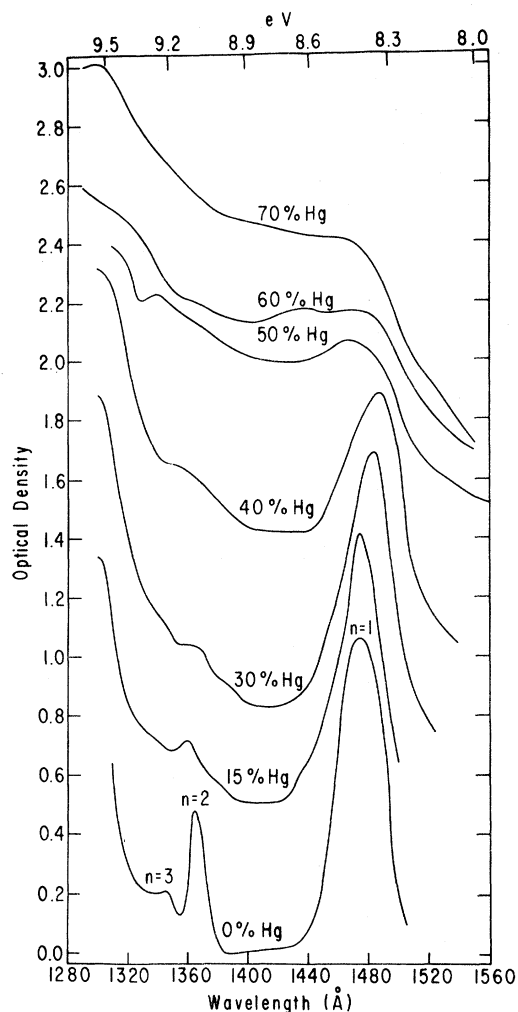


FIG. 1. Vacuum-uv absorption spectra of Hg/Xe solid films deposited at 40°K and measured at 10°K. The spectra were practically temperature independent in the range 10–40°K. The percentages represent the mole fractions of Hg. The spectra were vertically displaced on the optical density scale; the residual absorption at 1550 Å in each case was 0.1–0.2 optical-density units.

range $X_{\text{Hg}}=(40-60)\%$. However, in this concentration region a dramatic modification of the optical spectra takes place (Fig. 1), whereupon at 50% Hg appreciable line broadening occurs while at $X_{\text{Hg}}=60\%$ the excitonic spectrum is completely washed out. From these results we conclude that

(a) The disappearance of Wannier exciton states in Xe/Hg solid films occurring at $X_{\text{Hg}}=(55 \pm 5)\%$ is attributed to short-range screening in the metallic state.

(b) The present spectroscopic data indicate that the MNM transition is accompanied by a rather abrupt change in the bulk dielectric function of

the Xe/Hg system, rather than being due to the formation of metallic channels originating from percolation effects.

(c) Our spectroscopic criterion for the MNM transition in Xe/Hg films at $X_{\text{Hg}} \approx (55 \pm 5)\%$ implies that in this concentration region an abrupt increase in the electrical conductivity should take place. In recent studies^{6,18} of electrical conductivity of some divalent-metal/rare-gas solids (i.e., Pb/Ar and Cu/Ar films)¹⁸ an abrupt decrease of the electrical conductivity was observed at $\sim 60\%$ metal concentration.

(d) A rough estimate of the critical transition density to the metallic state is in order. Assuming a close packing of Xe atoms and of Hg^{+2} ions in the metallic phase ($X_{\text{Hg}} > 50\%$) the "critical" density of Hg atoms for the MNM transition is $\sim 9 \text{ g cm}^{-3}$ (i.e., number density $\sim 4.5 \times 10^{22} \text{ cm}^{-3}$). This density is very close to the critical density for the MNM transition in expanded subcritical and supercritical Hg at high temperature and pressures where Hall-effect¹⁹ data, the temperature coefficient of the electrical conductivity, and the thermoelectric power²⁰ indicate that the MNM transition in the one-component system occurs at the density of 9 g cm^{-3} .

(e) The condition⁹ for disappearance of bound electron-hole states due to short-range screening implies [see Eq. (4)] that $n^{1/3}a_H > 0.25$.⁹ Taking $\mathcal{C} = 2.5$ (the dielectric constant of Xe), $m^* = 1$, and $n = 4.5 \times 10^{22} \text{ cm}^{-3}$ at the onset of the metallic phase, we have $n^{1/3}a_H = 0.45$, so that the self-consistency condition (4) for short-range screening is satisfied, and exciton states should disappear in the metallic phase. It should be noted that the critical parameter $n^{1/3}a_H$ in the Xe/Hg system is somewhat higher than predicted on the basis of Eq. (4). It should, however, be borne in mind that Mott's estimate⁹ (4) for the critical density corresponding to the MNM transition due to long-range forces yields a result which is very similar to the prediction of the Hubbard-Mott electron correlation model.²¹ The latter scheme is inapplicable for a divalent metal such as Hg where the MNM transition originates from interband overlap effects²² (i.e., the Wilson model) rather than from correlation effects.

In Fig. 2 we present a schematic (one-electron) energy levels diagram for the Xe/Hg system.^{13,23-25} When the system becomes metallic ($X_{\text{Hg}} > 50\%$) the Hg *s* and *p* bands overlap, the Fermi energy is estimated as 5 eV (compared to 6.9 eV in liquid Hg). The broad structureless optical transition observed for $X_{\text{Hg}} > 50\%$ (see Fig. 1) may origi-

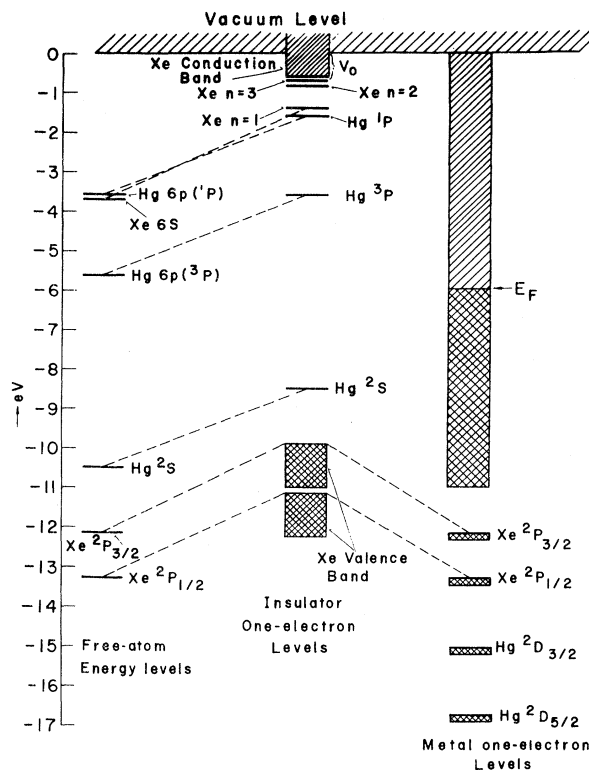


FIG. 2. Schematic one-electron energy-level diagrams for Hg/Xe solid mixtures in the insulating phase (low X_{Hg}) and in the metallic phase ($X_{\text{Hg}} \sim 55\%$).

inate from the following core excitations to the conduction-band states above the Fermi energy: (a) excitations from the Xe *5p* core states originating at ~ 7 eV and being split by the $\text{Xe}^+(^3P_{3/2})$ - $\text{Xe}^+(^2P_{1/2})$ spin-orbit coupling²³ (1.2 eV); (b) excitations from the Hg *5d* levels, which are expected to occur at ~ 9 eV and to be split by the $\text{Hg}^+(^2P_{3/2})$ - $\text{Hg}^+(^2D_{5/2})$ spin-orbit coupling (1.9 eV).²³

This work was supported by a grant from the Israeli National Council for Research and Development.

¹For a recent review see N. F. Mott and Z. Zinamon, Rep. Progr. Phys. **33**, 881 (1970).

²J. F. Morin, Phys. Rev. Lett. **3**, 34 (1959).

³J. Feinlieb and W. Paul, Phys. Rev. **155**, 841 (1967).

⁴H. Fritsche, J. Phys. Chem. Solids **6**, 69 (1959).

⁵J. C. Thompson, Rev. Mod. Phys. **40**, 704 (1968).

⁶R. C. Cate, J. G. Wright, and N. E. Cusack, Phys. Lett. **32A**, 467 (1970).

⁷F. Hensel and E. U. Franck, Rev. Mod. Phys. **40**, 697 (1968).

⁸U. Even and J. Jortner, Phys. Rev. Lett. **28**, 31 (1972).

⁹N. F. Mott, Phil. Mag. **6**, 287 (1967).

¹⁰W. Kohn, in *Solid State Physics*, edited by D. Turnbull and F. Seitz (Academic, New York, 1957), Vol. 5, p. 258.

¹¹J. Hermanson and J. C. Phillips, *Phys. Rev.* **150**, 652 (1966).

¹²E. Burstein, E. E. Bell, J. W. Davisson, and M. Lax, *J. Phys. Chem.* **57**, 840 (1953).

¹³G. Baldini, *Phys. Rev.* **128**, 1562 (1962).

¹⁴B. Raz and J. Jortner, *Proc. Roy. Soc., Ser. A* **317**, 113 (1970).

¹⁵N. Nagasawa, T. Nanba, and T. Karasawa, in *Proceedings of the Third International Conference on Vacuum UV Radiation*, Tokyo, 1971 (to be published).

¹⁶B. Raz, J. Magen, and J. Jortner, *Vacuum* **19**, 571 (1969).

¹⁷D. Onodera and Y. Toyozawa, *J. Phys. Soc. Jap.* **24**, 341 (1967); P. Soven, *Phys. Rev.* **156**, 809 (1967);

B. Velicky, S. Kirkpatrick, and H. Ehrenreich, *Phys.*

Rev. **175**, 747 (1968); J. Hoshen and J. Jortner, *J. Chem. Phys.* **56**, 933 (1972).

¹⁸J. G. Wright, A. Fatah, H. Endog, and N. E. Cusack, presented at the Chelsea Meeting on Amorphous Semiconductors, London, 1971 (to be published).

¹⁹U. Even and J. Jortner, *Phil. Mag.* **25**, 715 (1972).

²⁰R. W. Schmutzler and F. Hensel, to be published.

²¹J. Hubbard, *Proc. Roy. Soc., Ser. A* **281**, 401 (1964).

²²J. M. Ziman, *Principles of the Theory of Solids* (Cambridge Univ. Press, Cambridge, England, 1965), p. 80.

²³C. E. Moore, *Atomic Energy Levels as Derived from Analyses of Optical Spectra*, National Bureau of Standards Circular No. 467 (U. S. GPO, Washington, D. C., 1955).

²⁴J. F. O'Brien and K. J. Teegarden, *Phys. Rev. Lett.* **17**, 919 (1966).

²⁵W. B. Fowler, *Phys. Rev.* **151**, 657 (1966).

Direct-Process NMR Relaxation by Spin Waves in a One-Dimensional Antiferromagnet*

Peter M. Richards

Sandia Laboratories, Albuquerque, New Mexico 87115

(Received 24 March 1972)

Measurements of the proton relaxation time T_1 in $(\text{CH}_3)_4\text{NMnCl}_3$ are reported as a function of temperature between 4.0 and 1.2 K. Results are interpreted in terms of a direct relaxation process with spin waves in a one-dimensional antiferromagnet. They represent the first observation of direct-process NMR relaxation by magnons in any system and show that any gap in the spectrum at $q = \pi/a$ has to be less than 0.07 meV.

We report low-temperature NMR measurements of the proton longitudinal relaxation time T_1 in the one-dimensional antiferromagnet $(\text{CH}_3)_4\text{NMnCl}_3$ (TMMC). These are consistent with a direct-process coupling of the nuclear spin system to antiferromagnetic magnons. As such, they represent the first known observation of this kind of relaxation in a magnetic substance and verify the existence of a gapless spin-wave mode at the antiferromagnetic wave vector $q = \pi/a$ (a is the lattice spacing so that $q = 2\pi/2a$ is the reciprocal-lattice vector for the magnetic unit cell of an antiferromagnet). The latter verification is in accord with simple spin-wave theory and contrary to a recently proposed temperature-dependent gap by the author.¹ It also agrees with the theory of Lovesey and Meserve.²

Lively interest has centered around the existence³ of spin waves in a one-dimensional antiferromagnet. The standard antiferromagnetic spin-wave spectrum for an ordered system,⁴

$$\hbar\omega_q = 4JS|\sin qa|, \quad (1)$$

predicts a zero-frequency mode at $q = \pi/a$, and

whether this is appropriate for TMMC at finite temperature has been of particular concern. In Ref. 1 we noted that a second-order Green-function theory predicts a gap at $q = \pi/a \equiv q_0$ and that $\omega_{q_0} \propto T$, where T is the absolute temperature. This leads to a natural interpretation of static correlations^{5,6} at low temperature in terms of noninteracting spin waves. Parameters of the theory included nearest- and next-nearest-neighbor static correlation functions, which were obtained from the classical theory.⁶ Scales and Gersch⁷ have since shown that a self-consistent solution for quantum spins produces a gap at q_0 even for $T = 0$. Lovesey and Meserve,² on the other hand, have used a continued fraction expansion which allows for damping—something absent in the treatments of Refs. 1 and 7. They find the $q = \pi/a$ mode to be strongly peaked at $\omega = 0$ for temperatures below about 20 K in TMMC.

Inelastic neutron scattering data³ exist for $q^*a \geq 0.05\pi$, where $q^* = \pi/a - q$, at temperatures down to 1.9 K. At $q^*a = 0.05\pi$ the observed magnon energy is 1 meV. Since the predicted gap energy of Ref. 1 is 0.1 meV at 1.9 K, and that of Ref. 7 is